Structure and Physical Properties of Syndiotactic Polypropylene Oriented from Different Polymorphs

Liberata Guadagno, Concetta D'Aniello, Carlo Naddeo, and Vittoria Vittoria*

Dipartimento di Ingegneria Chimica e Alimentare, Università di Salerno, Via Ponte Don Melillo, 84084 Fisciano (Sa), Italy

Received November 14, 2000; Revised Manuscript Received February 1, 2001

ABSTRACT: Two syndiotactic polypropylene (sPP) samples were obtained by quenching the melt in a bath at 0 °C for 1 min (sample **1A**, crystallized in the helical form I), and for 3 days (sample **1B**, in the trans-planar mesophase). Samples **1A** and **1B** were drawn at room temperature obtaining fibers with draw ratios $\lambda = 5$, 6, and 7. The fibers were analyzed under stress by X-rays and FTIR, successively unhooked, and again analyzed. Different structural organizations were found in the fibers fixed or relaxed. In sample **1B**, the drawing produced a progressive orientation of the trans-planar mesophase ending with the formation of the crystalline trans-planar form III. On releasing the tension, form III transformed again into the trans-planar mesophase, but very weak helical reflections appeared in the X-ray patterns. Infrared spectra confirmed that one of the helical bands increases on releasing the tension. In sample **1A**, the helical form I was first oriented and then, by progressive drawing, transformed into the crystalline trans-planar form III. Releasing the tension, form III again converted into the helical form I and partially into the trans-planar mesophase. Despite the different structural organizations, all the relaxed fibers showed a good elasticity and the same qualitative behavior. It is characterized for all the fibers by a low hysteresis and a small permanent set after a 50% deformation. However, the elastic fibers show a much higher modulus than the conventional elastomers.

Introduction

The use of new metallocene catalysts in recent years has allowed a very rapid development of polymers with a wide range of structures and related properties, renewing the interest in polymers whose behavior had not been well understood. Among them, syndiotactic polypropylene (sPP), recently obtained with high tacticity and high molecular weight,[1−3] is receiving a great attention owing to its new properties respect to the isotactic isomer (iPP). In the case of sPP the difficulty of correlating the physical properties to the structural organization is principally due to its very complex polymorphic behavior, not yet fully clarified.[4−20]

Four crystalline forms of sPP have been described so far. Forms I and II are characterized by chains in a $(T_2G_2)_n$ helical conformation,[4,10] whereas forms III and IV present chains in trans-planar and $(T_6G_2T_2G_2)_n$ conformations,[8−9] respectively. Form I is the stable form of sPP obtained under the most common conditions of crystallization either from the melt state or from solution as single crystals.[4−7,13] In this form, the helical chains are packed, in the limit-ordered structure, with an alternation of right-handed and left-handed helices along both axes of the unit cell, that is othorhombic with axes $a = 14.50$ Å, $b = 11.20$ Å, and $c = 7.45$ Å. Disorder in this regular alternation is present in samples crystallized from the melt at low temperatures: in this case the unit cell is orthorhombic with axes $a = 14.50$ Å, $b = 5.60$ Å, and $c = 7.45$ Å.

Form II corresponds to the *C*-centered structure in which the helical chains have the same chirality. It was obtained by stretching at room-temperature compression molded specimens of sPP samples with low stereoregularity.[4,10] The trans-planar form III is the metastable polymorph of sPP. It is obtained through cold drawing of sPP samples, quenched from the melt at low temperatures.[8] Recently, the spontaneous crystallization of an unoriented trans-planar form was reported, keeping the sPP, after melting, in a bath at 0 °C for a long time.[20−21] This form was interpreted as the crystalline form III,[20] or as a mesophase, or also a paracrystalline, disordered phase, containing lateral disorder in the packing of the trans-planar chains. This phase, stable up to 80 °C, is almost completely transformed into the more stable form I at higher temperatures.[21]

The crystallization conditions of sPP from the melt at low temperatures are very critical. When sPP, rapidly quenched from the melt in a bath at 0 °C, is extracted at room temperature after a short time (for example 1 min), it is elastic due to a very low crystallinity; however, the elastic behavior is soon lost for the rapid crystallization in the helical form I. At variance, when sPP is drawn at room temperature and the tension is released, it shows a very interesting elasticity along the draw direction, depending on the particular structure of the oriented sample.[22−25] This result is very important in the light of the growing need for materials offering the properties and performances of rubber. In addition, whereas rubbery materials have a very low modulus, less than 1 MPa, the elastic fibers of sPP show a modulus of some order of magnitude higher. The behavior of oriented sPP is very reminiscent of the so-called "hard elastic fibers" of isotactic polypropylene, investigated many years ago.[26−29] In that case, the elasticity was correlated to the row-nucleated morphology, due to the particular processing conditions. In the case of sPP it is not yet clear the origin of the elastic behavior. It is therefore important to study both the structure and the morphology of oriented sPP samples, to try to understand it.

In a previous paper, we analyzed a fiber drawn from form I at room temperature[24] and observed that the elastic behavior was closely correlated to the conformational transition between the trans-planar and the helical conformations.

10.1021/ma0019398 CCC: $20.00
Published on Web 03/15/2001

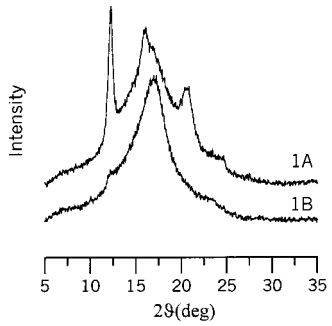

Figure 1. X-ray powder diffractograms of samples **1A** and **1B**.

In this paper, we have studied fibers drawn from different initial structures at different draw ratios. In particular we oriented samples with initial either helical or trans-planar conformation of the chains, obtaining fibers with different structural organization. The structure was investigated before and after releasing the tension, because in this range the fibers show elastic behavior. The elasticity was investigated through the hysteresis cycles at room temperature.

Experimental Section

The syndiotactic polypropylene was synthesized according to a previous procedure.[30] The polymer was analyzed by ^{13}C NMR spectroscopy at 120 °C on an AM 250 Bruker spectrometer operating in the FT mode at 62.89 MHz, by dissolving 30 mg of sample in 0.5 mL of $C_2D_2Cl_4$. Hexamethyldisiloxane was used as an internal chemical shift reference. The reaction resulted in a polymer composed of 91% syndotactic pentads.

The sPP powders were molded in a hot press, at 150 °C, forming a film 0.1 mm thick, and rapidly quenched at 0 °C in an ice−water bath. One sample was extracted from the bath after 1 min (sample **1A**). Another sample was kept in the cold bath for 3 days (sample **1B**).

Sample **1A** and sample **1B** were drawn up to $\lambda = 5$, 6, and 7 (samples **5A**, **6A**, and **7A** and samples **5B**, **6B**, **7B**, respectively) at room temperature, using a dynamometric apparatus INSTRON 4301. The deformation rate was 10 mm/min, and the initial length of the sample was 10 mm. The drawn samples were analyzed by X-rays and FTIR, under tension, before unhooking. Afterward they were unhooked and again analyzed (samples **5AR**, **6AR**, **7AR** and **5BR**, **6BR**, **7BR**, respectively).

Fiber diffraction spectra were recorded under vacuum by means of a cylindrical camera with a radius of 57.3 mm and the X-ray beam direction perpendicular to the fiber axis (V-filtered Cr Kα radiation). The imaging plate Fujix BAS-1800 system was used to record the diffraction patterns. The X-ray profile of sample **6AR** was decomposed in the single reflections using a Lorentzian fitting.

The infrared spectra were obtained in absorbance by using a FTIR−Bruker IFS66 spectrophotometer with a resolution of 4 cm^{-1} (32 scans collected).

The elastic behavior of the unhooked fibers was analyzed through the hysteresis cycles,[31] performed in the Instron at room temperature. The initial rate of deformation was 10 mm/min.

Results and Discussion

Unoriented Samples. The X-ray powder diffraction patterns of samples **1A** and **1B**, are shown in Figure 1. The diffractogram of sample **1A** indicates that this sample crystallized in the usual form I, characterized by the most intense peaks at 12.3, 15.9, and 20.8° of 2ϑ. The absence of the (211) reflection at $2\vartheta = 18.9°$ indicates that we obtained a disordered modification of form I, as expected for a sample rapidly quenched to 0 °C. In this case, as well documented in other cases, departures from the fully antichiral packing both along *a* and *b* axes may occur, leading to a less ordered form. The preferential crystallization of this disordered form was always found in samples of low syndiotacticity or in powder samples crystallized from the melt at low temperatures.[10]

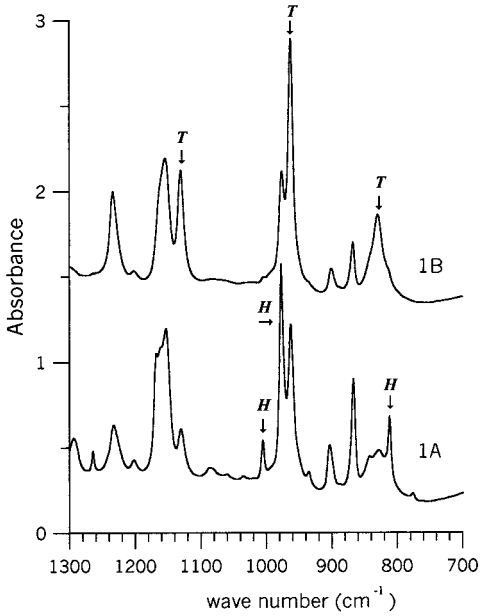

Figure 2. FTIR spectra in absorbance (1300−700 cm^{-1}) of samples **1A** and **1B**, in which the arrows indicate the helical (H) and the trans-planar (T) peaks.

The diffractogram of sample **1B**, kept at 0 °C for 3 days, shows a broad peak centered around $2\vartheta = 17°$, with a shoulder around $2\vartheta = 24°$. Nakaoki et al.[20] identified these reflections as characteristic of form III, having the chains in trans-planar conformation. At variance, we suggested that this new phase, stabilized at low temperature for a long time, although correctly characterized by chains in trans-planar conformation, could not be identified as the known crystalline form III: it should be rather identified as a mesophase, or also a paracrystalline, disordered phase, containing lateral disorder in the packing of the trans-planar chains.[21]

To confirm that samples **1A** and **1B** have the chains in different conformations, that is helical in sample **1A** and trans-planar in sample **1B**, in Figure 2 we report the FTIR spectra in absorbance (1300−700 cm^{-1}) of the two samples. Infrared analysis is very sensitive for the chain conformation determination: as a matter of fact helical and trans-planar bands have been evidenced since the first preparation of the syndiotactic isomer of polypropylene.[32,33] We observe that, in sample **1A**, the bands of the helical form of sPP, appearing at 810, 977, and 1005 cm^{-1}, are very evident and well developed. At variance, in sample **1B**, the helical bands are absent, or strongly reduced, whereas the bands corresponding to long strands in trans-planar conformation, appearing at 831, 963, and 1132 cm^{-1}, are very evident and well developed. This confirms that sample **1B**, kept in the cold bath for 3 days, assumed a prevalently trans-planar conformation. However, the presence of the helical band at 977 cm^{-1} indicates that a small fraction of chains in helical conformation was formed too, probably upon removing the sample from the cold bath. This is confirmed by a small trace, in the diffractogram of

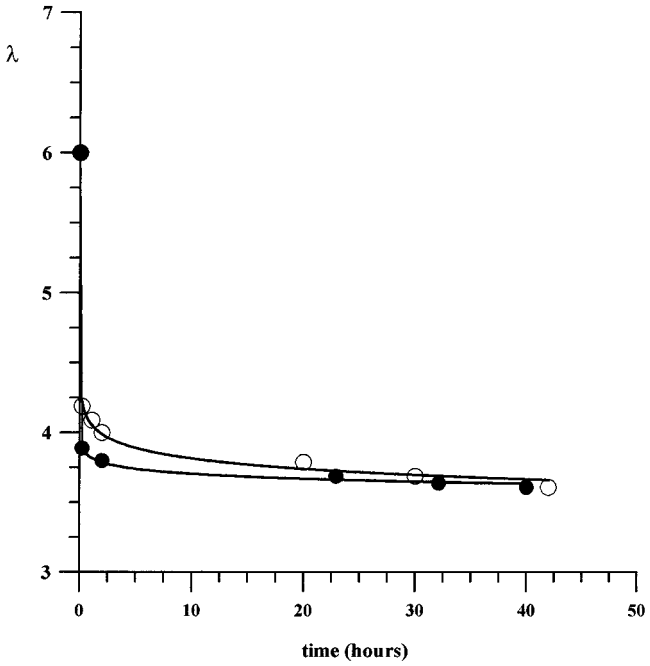

Figure 3. Shrinkage of samples **6A** (●) and **6B** (○) as a function of the time after unhooking.

Table 1. Shrinkage of sPP Fibers

sample	$(l_\lambda - l_1)/l_\lambda \times 100$
5BR	33
6BR	33
7BR	33
5AR	33
6AR	37
7AR	38

sample **1B** (see Figure 1), of the reflection at $2\vartheta = 12.3°$, corresponding to the (200) reflection of the helical form I.

On the other hand, in sample **1A**, the trans-planar bands at 831, 963, and 1132 cm^{-1}, are present too, although of reduced intensity with respect to sample **1B**. This means that the permanence in the bath at 0 °C, even for 1 min, produced also in sample **1A** a small formation of a mesophase with chains in a trans-planar conformation. This is also confirmed by the broadening of the (010) reflection at $2\vartheta = 15.9°$, with a prominent shoulder at $2\vartheta = 17°$, typical of the trans-planar mesophase (see Figure 1).

Shrinkage of the Oriented Samples. Samples **1A** and **1B** were drawn at $\lambda = 5$, 6, and 7 and unhooked after 18 h. When the tension on the fibers was released, they underwent a large shrinkage.

In Figure 3 the shrinkage of the fibers **6A** and **6B** is shown as a function of time. For each sample the major part of the shrinkage occurs as soon as they are unhooked, whereas a further small contraction during the permanence at room temperature can be observed. In any case the fibers were analyzed soon after releasing the tension, when the most part of shrinkage had occurred.

The shrinkage of all the fibers is reported in Table 1, as $(l_\lambda - l_1)/l_\lambda \times 100$, where l_λ is the length before unhooking and l_1 is the length just after unhooking. We observe that for **B** fibers the shrinkage is the same at each draw ratio, whereas in the case of **A** fibers the higher the initial draw ratio the higher the successive shrinkage. Furthermore, the fibers obtained from samples **A** and **B** show a similar value of retraction, being slightly higher the first.

In the interval between l_1 and l_λ the fibers show elastic behavior: therefore, we thoroughly investigated the structural organization before and after unhooking.

Oriented Sample B. In Figure 4 we show the X-ray fiber diffraction patterns of the oriented samples before (**5B**, **6B**, and **7B**) and after releasing the tension (**5BR**, **6BR**, and **7BR**). They were drawn from sample **1B** having the chains in trans-planar conformation. In Table 2 all the reflections, the spacings and the corresponding 2ϑ with the *hkl* indices for the helical and trans-planar forms are reported.

The pattern **5B**, relative to $\lambda = 5$ under tension, indicates that the sample is already well oriented, although not completely. On the equator, we observe a polarized reflection, corresponding to the same diffraction angle as the starting sample **B**. Therefore, it is the trans-planar mesophase, oriented during the drawing. In confirmation of this, on the first layer we observe a medium intensity reflection corresponding to an identity period of 5.05 Å: it is the (021) reflection of the trans-planar form, indicating that the mesophase is a precursor of the crystalline trans-planar form III. Neither on the equator nor on the first layer we observe helical reflections: they were present in the sample drawn at $\lambda = 4$, as a residual of the small helical fraction in the starting sample,[23] but have disappeared with further drawing.

The pattern **5BR**, relative to sample $\lambda = 5$ after releasing the tension, shows the same reflections as before, although less concentrated, as if the unhooked sample partially had lost orientation. At the same time, very weak reflections, both on the equator ($2\vartheta_{Cu} = 12.3°$) and on the first layer ($2\vartheta_{Cu} = 20.9°$), characteristic of the helical form, are now observable.

Going to the successive draw ratio, sample **6B** under tension, we observe that the previous equatorial reflection is split in two well polarized reflections, corresponding to the crystalline form III. They are the (020) and (110) reflections, reported by Chatani.[8] On the equator also the reflection (130) of the same structure appears. On the first layer there is only one reflection, the (021) of the trans-planar form, sharper and strong.

The pattern of the released sample **6BR** shows that the two polarized reflections of the crystalline form III again converged in the polarized reflection of the trans-planar mesophase, confirming that the mesophase tends toward the crystalline form III when it is under tension, whereas form III transforms into the oriented mesophase when the tension is released. The reflection corresponding to the trans-planar form is evident on the first layer, too. As in the previous sample, very weak helical reflections are observable both on the equator and on the first layer, but they are even weaker, almost indistinguishable.

In the sample drawn to $\lambda = 7$ and analyzed under tension, the structure of form III is well developed, and besides the three reflections on the equator, two reflections on the first layer corresponding to (021) and (111) planes of form III are now quite well observable. The relaxed sample **7BR** is very similar to the previous **6BR**. The two equatorial reflections of form III converged into the reflection of the mesophase, but now the weak reflection (130) is still present. On the first layer, one of the two reflections has disappeared and we can observe only the (021) reflection of the trans-planar

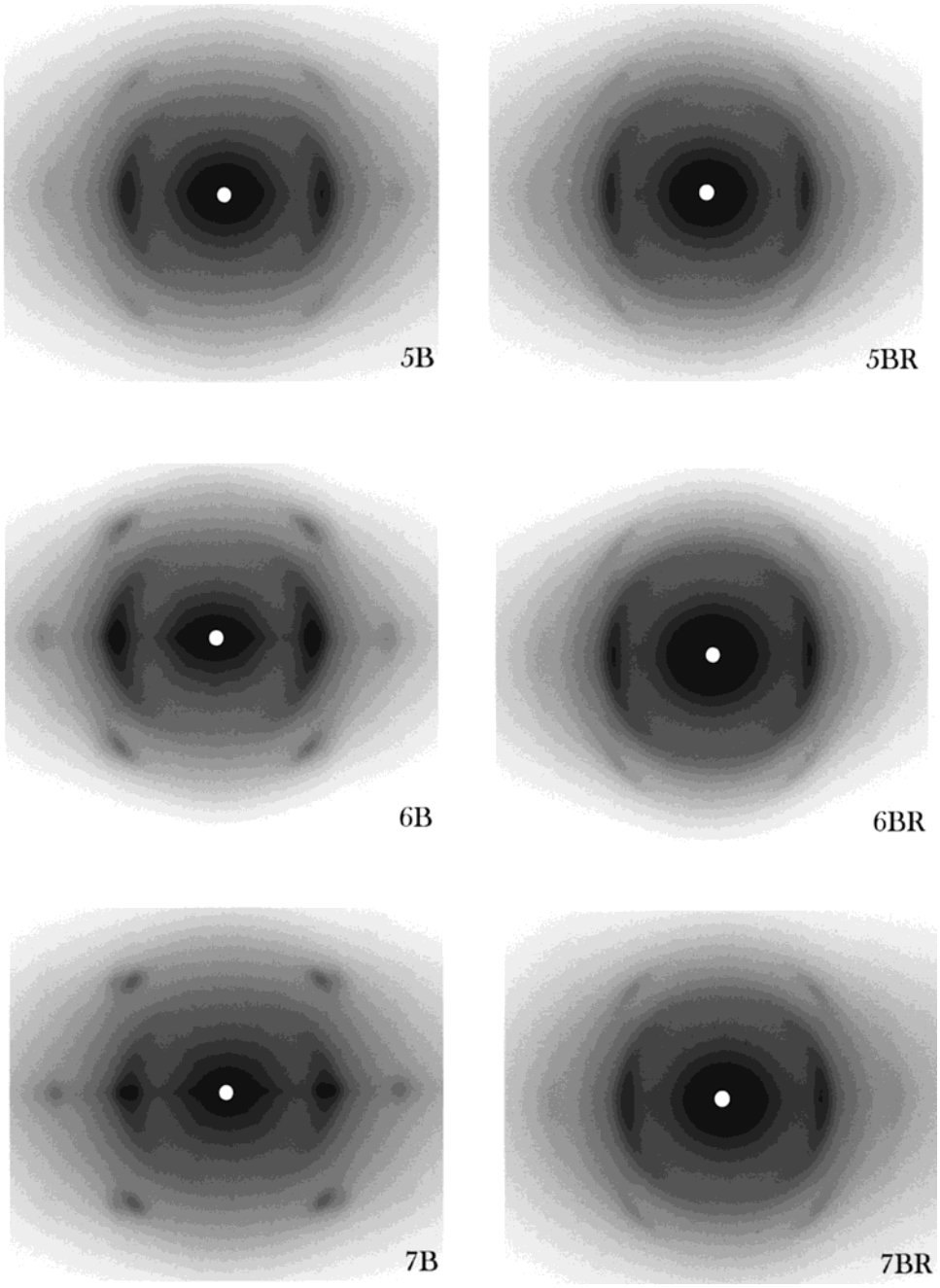

Figure 4. X-ray fiber diffraction patterns of the fibers with draw ratios $\lambda = 5$, $\lambda = 6$, and $\lambda = 7$ before (**5B**, **6B**, and **7B**) and after (**5BR**, **6BR**, and **7BR**) releasing the tension.

form, appearing more diffuse. The helical reflections have almost disappeared.

From these results, we can conclude that, by drawing the trans-planar mesophase, we first obtain its orientation and, successively, increasing the stress on the sample, the transformation of the oriented trans-planar domains into the crystalline form III, which appears well developed and oriented in the sample drawn at $\lambda = 7$ and analyzed under tension. On releasing the tension, form III, which is stable only under tension, loses the lateral packing and transforms into the oriented mesophase. However, the presence of less intense helical reflections, not present in the fixed fibers, suggests that a small fraction of the oriented trans-planar phase, on relaxing, transformed into the oriented helical form.

The infrared analysis confirms the results of X-rays. In Figure 5 we show the FTIR spectra of fibers before (**5B**, **6B**, and **7B**) and after the release of the tension (**5BR**, **6BR**, **7BR**). In all the fixed fibers, the trans-planar bands, appearing at 831, 963, and 1132 cm^{-1}, are present and well developed as well as they were in the starting sample **B** (see Figure 2). It is interesting to note that the trans-planar band at 831 cm^{-1} is split into two bands when the crystalline form III is formed.

Considering now the helical bands, we observe that the 810 and 1005 cm^{-1} bands are completely absent, whereas the 977 cm^{-1} band appears only as a shoulder of the trans planar band at 963 cm^{-1}. As far as the fixed fibers are considered, we can affirm that the helical chains are absent in the FTIR spectra. In the unhooked fibers, we observe a slight increase of the band at 977 cm^{-1} in all the released samples and the appearance of the 810 cm^{-1} as a shoulder only in sample **5BR**. Evidently, the critical length sequence in helical conformation for the bands at 810 and 1005 cm^{-1} is not

Table 2. Reflections Observed in the X-ray Fibers Diffraction Spectra of Sample B

sample	period along chain axis (Å)	2θ, deg (Cu)	dist (Å)	I	*hkl*[a]
5B (fiber $\lambda = 5$)		16.0−18.0		vs	*b*
		29.47	3.03	vw	130 form III
	5.05	23.73	3.75	ms	021 form III
6B (fiber $\lambda = 6$)		15.87	5.58	vs	020 form III
		18.76	4.73	vs	110 form III
		29.47	3.03	ms	130 form III
	5.05	23.73	3.75	s	021 form III
7B (fiber $\lambda = 7$)		15.87	5.58	vs	020 form III
		18.76	4.73	vs	110 form III
		29.47	3.03	ms	130 form III
	5.05	23.73	3.75	s	021 form III
		25.78	3.46	ms	111 form III
5BR (relaxed fiber $\lambda = 3.3$)		12.32	7.18	vw	200 form I[c]
					200 form I[d]
		∼17.0	5.21	s	trans-planar mesophase
	7.45	20.86	4.26	vvw	111 form I[c]
					121 form I[d]
	5.05	23.73	3.75	m	021 form III
6BR (relaxed fiber $\lambda = 4.0$)		12.32	7.18	vw	200 form I[c]
					200 form I[d]
		∼17.0	5.21	s	trans-planar mesophase
	7.45	20.86	4.26	vvw	111 form I[c]
					121 form I[d]
	5.05	23.73	3.75	m	021 form III
7BR (relaxed fiber $\lambda = 4.7$)		12.32	7.18	vvw	200 form I[c]
					200 form I[d]
		∼17.0	5.21	s	trans-planar mesophase
	7.45	20.86	4.26	vvw	111 form I[c]
					121 form I[d]
	5.05	23.73	3.75	m	021 form III

[a] Crystalline forms where the reflection is allowed. [b] For the interpretation refer to the text. [c] Form I orthorhombic unit cell with axes $a = 14.50$ Å, $b = 5.60$ Å, and $c = 7.45$ Å. [d] Form I orthorhombic unit cell with axes $a = 14.50$ Å, $b = 11.20$ Å, and $c = 7.45$ Å.

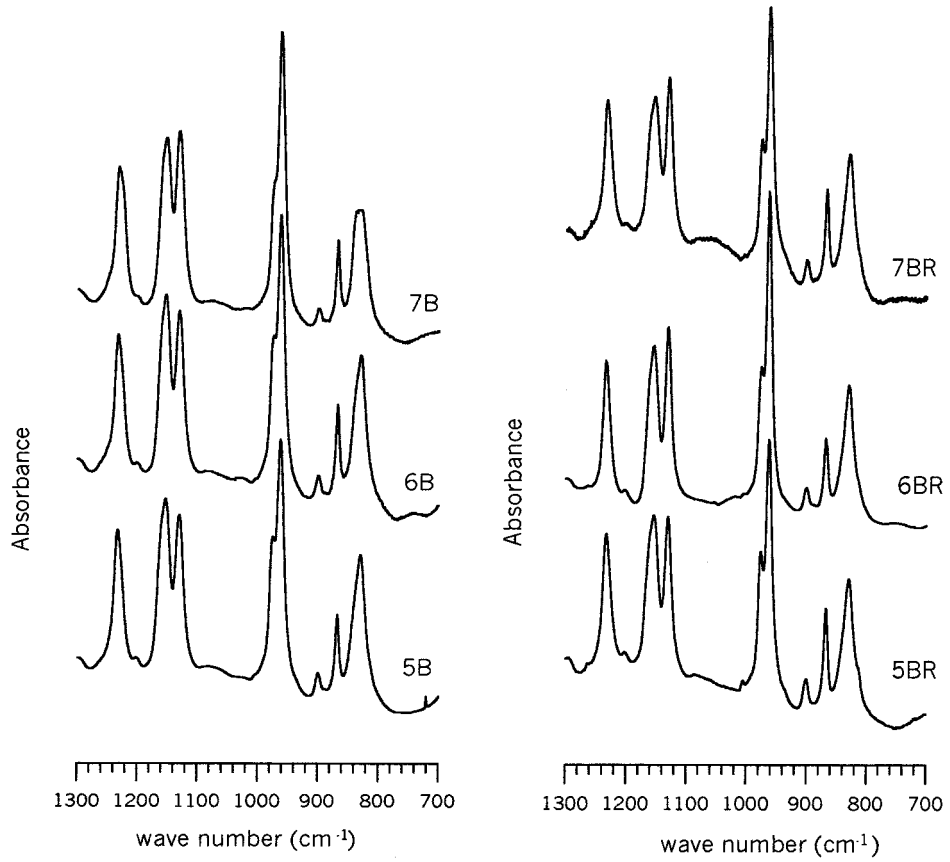

Figure 5. FTIR spectra in absorbance (1300−700 cm^{-1}) of the fibers with draw ratios $\lambda = 5$, $\lambda = 6$, and $\lambda = 7$ before (**5B**, **6B**, and **7B**) and after (**5BR**, **6BR**, and **7BR**) releasing the tension.

reached, and this confirms that the helical form that appears in the relaxed fibers is very poorly crystalline, if any crystallinity is present, as shown also by the X-rays.

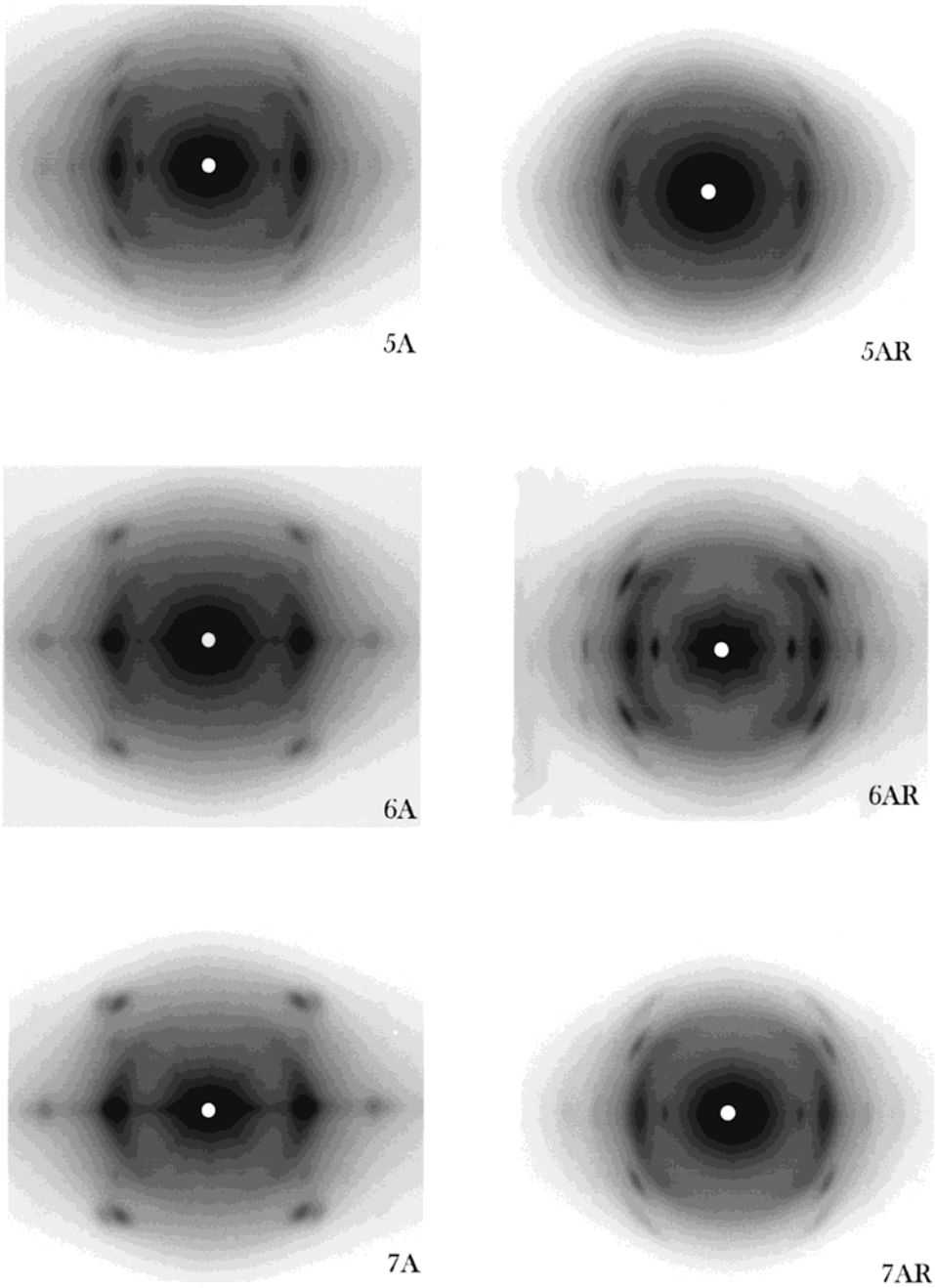

Figure 6. X-ray fiber diffraction patterns of the fibers with draw ratios $\lambda = 5$, $\lambda = 6$, and $\lambda = 7$ before (**5A**, **6A**, and **7A**) and after (**5AR**, **6AR**, and **7AR**) releasing the tension.

Oriented Sample A. In Figure 6 we show the X-ray fiber diffraction patterns of the fibers before (**5A**, **6A**, and **7A**) and after releasing the tension (**5AR**, **6AR**, and **7AR**). All the reflections, the spacing, and the corresponding 2ϑ, with the indices hkl of the allowed forms, are reported in Table 3. First of all, we observe that the sample drawn at a draw ratio of 5 is already well oriented. On the equator the first strong spot corresponds to the (200) reflection of the helical form I. The second spot, very strong, could be the superposition of the (010) reflection of the helical form I and the reflection of the trans-planar mesophase that is formed during the drawing process. The presence of a trans-planar form is confirmed on the first layer (see later). The third weak spot corresponds to the (400) reflection of the helical form, whereas the fourth, very weak, is correspondent to the (130) reflection of the trans-planar form. On the first layer we observe a strong reflection, corresponding to an identity period of 7.45 Å: it can be indexed as (111) of the disordered form I. Another weaker but well-distinguishable reflection, corresponding to an identity period of 5.05 Å, is indexed as a reflection (021) of the trans-planar form. The unhooked fiber **5AR** partially lost orientation, and all the reflections appear weaker; some of them are hardly distinguishable. In particular, all the previous helical reflections are still present, although weaker and less oriented, whereas the reflection of the trans-planar form is present in the second spot of the equator; a weak residual reflection on the first layer is also present.

In the pattern of the sample drawn at $\lambda = 6$ under tension, the helical reflections, either the (200) on the equator, or the (111) on the first layer are very much reduced respect to sample **5AR**, almost indistinguishable, whereas the reflections of the trans-planar form are strong and well resolved. Indeed, the second spot

Table 3. Reflections Observed in the X-ray Fibers Diffraction Spectra of Sample A

sample	period along chain axis (Å)	2θ, deg (Cu)	dist (Å)	I	*hkl*[a]
5A (fiber $\lambda = 5$)		12.32	7.18	vs	200 form I[c]
					200 form I[d]
		15.4−18.4		s	*b*
		24.79	3.59	w	400 form I[c]
					400 form I[d]
		29.47	3.03	vvw	130 form III
	7.45	20.86	4.26	ms	111 form I[c]
					121 form I[d]
	5.05	23.73	3.75	mw	021 form III
6A (fiber $\lambda = 6$)		12.32	7.18	vw	200 form I[c]
					200 form I[d]
		15.87	5.58	vs	020 form III
		18.76	4.73	vs	110 form III
		29.47	3.03	w	130 form III
	7.45	20.86	4.26	w	111 form I[c]
					121 form I[d]
	5.05	23.73	3.75	ms	021 form III
		25.78	3.46	w	111 form III
7A (fiber $\lambda = 7$)		15.87	5.58	vs	020 form III
		18.76	4.73	vs	110 form III
		29.47	3.03	mw	130 form III
	7.45	20.86	4.26	vvw	111 form I[c]
					121 form I[d]
	5.05	23.73	3.75	s	021 form III
		25.78	3.46	ms	111 form III
5AR (relaxed fiber $\lambda = 3.3$)		12.32	7.18	vs	200 form I[c]
					200 form I[d]
		15.7−18.2		s	*b*
		24.79	3.59	m	400 form I[c]
					400 form I[c]
	7.45	20.86	4.26	s	111 form I[c]
					121 form I[d]
		27.38	3.26	mw	311 form I[c]
					321 form I[d]
	5.05	23.73	3.75	mw	021 form III
6AR (relaxed fiber $\lambda = 3.8$)		12.32	7.18	vs	200 form I[c]
					200 form I[d]
		15.7−18.2		s	*b*
		24.79	3.59	ms	400 form I[c]
					400 form I[d]
	7.45	20.86	4.26	s	111 form I[c]
					121 form I[d]
		27.38	3.26	mw	311 form I[c]
					321 form I[d]
	5.05	23.73	3.75	mw	021 form III
7AR (relaxed fiber $\lambda = 4.3$)		12.32	7.18	vs	200 form I[c]
					200 form I[d]
		15.78−18.2		s	*b*
		24.79	3.59	mw	400 form I[c]
					400 form I[d]
	7.45	20.86	4.26	s	111 form I[c]
					121 form I[d]
		27.38	3.26	vvw	311 form I[c]
					321 form I[d]
	5.05	23.73	3.75	mw	021 form III

[a] Crystalline forms where the reflection is allowed. [b] For the interpretation refer to the text. [c] Form I orthorhombic unit cell with axes $a = 14.50$ Å, $b = 5.60$ Å, and $c = 7.45$ Å. [d] Form I orthorhombic unit cell with axes $a = 14.50$ Å, $b = 11.20$ Å, and $c = 7.45$ Å.

on the equator is now split in two reflections, corresponding to the (020) and (110) reflections of the trans-planar form III, described by Chatani.[8] On the first layer, the reflection (021) corresponding to the identity period of 5.05 Å (trans-planar form III) is now much stronger than that of 7.45 Å. Therefore, as in the previous case of sample **B**, at this draw ratio we observe the appearance of the crystalline form III, although not yet completely ordered. The unhooked sample **6AR** shows a transition from the trans-planar form III to both the oriented helical and trans-planar form. The reflections of the oriented helical form I are present on the equator as well as in the first layer. The oriented trans-planar mesophase shows a strong reflection on the equator, superimposed to the second helical reflection, and still a weak reflection on the first layer, corresponding to the (021) reflection with an identity period of 5.05 Å.

In the sample **7A** drawn at $\lambda = 7$ the reflections of the crystalline form III are very intense and well resolved. Only a very weak reflection of the helical form is still present on the first layer. Therefore, at this draw ratio we obtained the almost complete transformation into the crystalline trans-planar form III. However, as we have seen in the previous case, this crystalline form is stable only if the sample is maintained under tension. As a matter of fact, after releasing the tension, sample **7AR** shows the transition from form III to either the

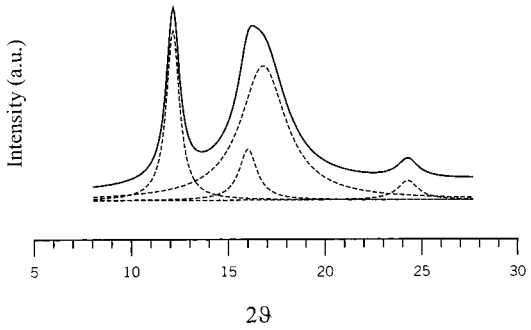

Figure 7. Equatorial scan of the X-ray pattern intensity for sample **6AR**: dotted lines correspond to the peaks obtained by deconvolution using Lorentzian fitting.

helical form I or the trans-planar mesophase. In fact, as in the previous case, we observe on the equator the reflections corresponding to the (200), (010), and (400) of the oriented form I and on the first layer the reflection (111) of form I. The reflection of the oriented mesophase is present on the equator, joined to that of the helical form, and on the first layer, that is the reflection indexed as (021) of the trans-planar form, corresponding to an identity period of 5.05 Å.

The second peak on the equator, extending in the range 15.7−18.2° of 2ϑ, was resolved by performing an equatorial scan of the intensity profile and a deconvolution. The X-ray profile was decomposed in the single reflections using a Lorentzian fitting. The original peak and the peaks after the deconvolution, for sample **6AR**, are shown in Figure 7. The original broad peak shows its maximum at 15.9° of $2\vartheta_{Cu}$ and a pronounced shoulder at 17° of $2\vartheta_{Cu}$. The deconvolution clearly shows two peaks, the first being at 15.9° of $2\vartheta_{Cu}$, corresponding to the helical form I, and the second at 17° of $2\vartheta_{Cu}$, corresponding to the trans-planar mesophase. Moreover, the intensity of the peak at 15.9° of $2\vartheta_{Cu}$ is in the right ratio respect to the peak at 12.3° of $2\vartheta_{Cu}$ for the helical form I. Therefore, there is no doubt that, in our case, form III transformed partially into form I and partially into the trans-planar mesophase.

In Figure 8 we show the FTIR spectra of all the fibers before and after releasing the tension. Compared to the fibers obtained drawing sample **B**, in the case of sample **A** the fiber drawn at $\lambda = 5$ and analyzed under tension still shows the helical bands at 810 and 977 cm^{-1}, although of very reduced intensity. All the trans-planar bands are all very well developed and intense. In the fibers **6A** and **7A**, we observe a further decrease of the helical bands: they disappear when form III is completed. In fact in sample **7A** the band at 810 cm^{-1} is not present and that at 977 cm^{-1} appears only as a shoulder. Also in this case we observe that in the spectrum of form III the trans-planar band at 831 cm^{-1} is split in two peaks at 829 and 837 cm^{-1}.

This observation is very interesting since it allows one to reveal the presence of the crystalline form III by infrared analysis and to distinguish, by infrared analysis, between the crystalline form III and the trans-planar mesophase.

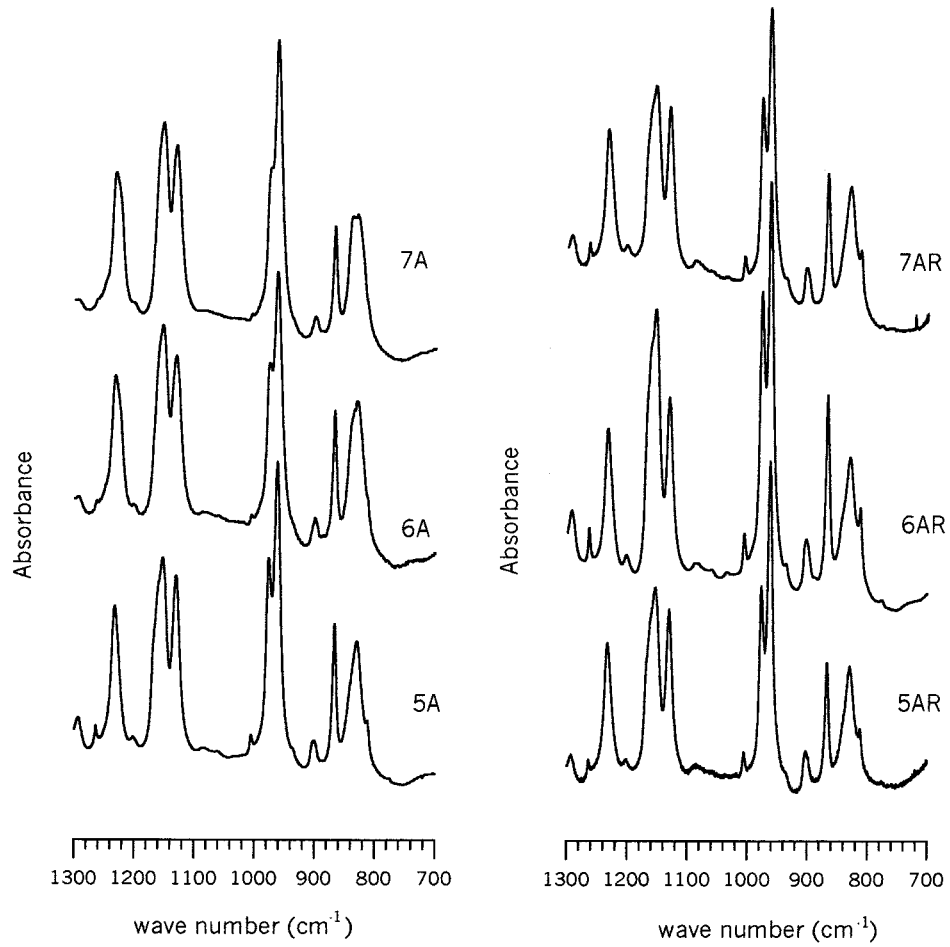

Figure 8. FTIR spectra in absorbance (1300−700 cm^{-1}) of the fibers with draw ratios $\lambda = 5$, $\lambda = 6$, and $\lambda = 7$ before (**5A**, **6A**, and **7A**) and after (**5AR**, **6AR**, and **7AR**) releasing the tension.

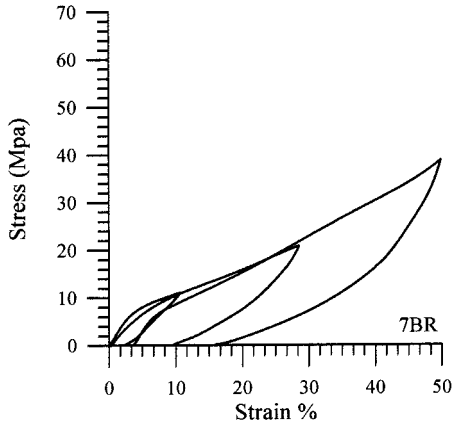

Figure 9. Hysteresis cycles of sample **7BR**.

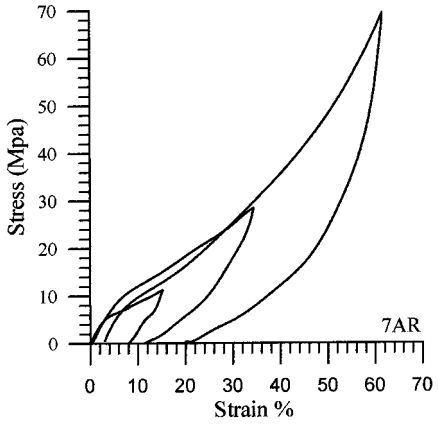

Figure 10. Hysteresis cycles of sample **7AR**.

Table 4. Mechanical Parameters for sPP Fibers Submitted to Hysteresis Cycles

	set %			dissipated energy (MPa)		
sample	primary cycle	secondary cycle	tertiary cycle	primary cycle	secondary cycle	tertiary cycle
5BR	3	7	18	55	181	330
6BR	5	11	17	63	189	363
7BR	2	9	16	39	199	539
5AR	6	10	20	113	334	721
6AR	6	11	20	63	199	847
7AR	9	12	22	72	326	1015

In the spectra of the relaxed fibers **5AR**, **6AR**, and **7AR**, the trans-planar bands do not decrease in intensity, and we observe in addition only a small increase of the helical bands at 810 and 977 cm^{-1}. The two bands of form III again converge into the 831 cm^{-1} trans-planar band, indicating the transformation of the crystalline form III into the mesophase.

The combined results of X-rays and FTIR indicate that the helical form I is progressively oriented during drawing and gradually transforms into the trans-planar structure. At a draw ratio of 7, this transformation is almost complete. When the crystalline form I is subjected to a progressively increasing stress, the chains undergo a transition between helix to trans-planar, breaking the crystals and creating a new phase with the chains in trans-planar conformation. This effect during drawing is well explainable by a stress-induced conformational transition, already described for other systems. As example, it was reported that by drawing the α-phase poly(vinylidene fluoride) (PVF_2) with chains in tg^+tg^- conformation, the *β*-phase with the chains in trans-planar conformation was obtained.[34] Also syndiotactic polystyrene, drawn when the chains are in helical conformation, undergoes a conformational transition into the trans-planar form.[35]

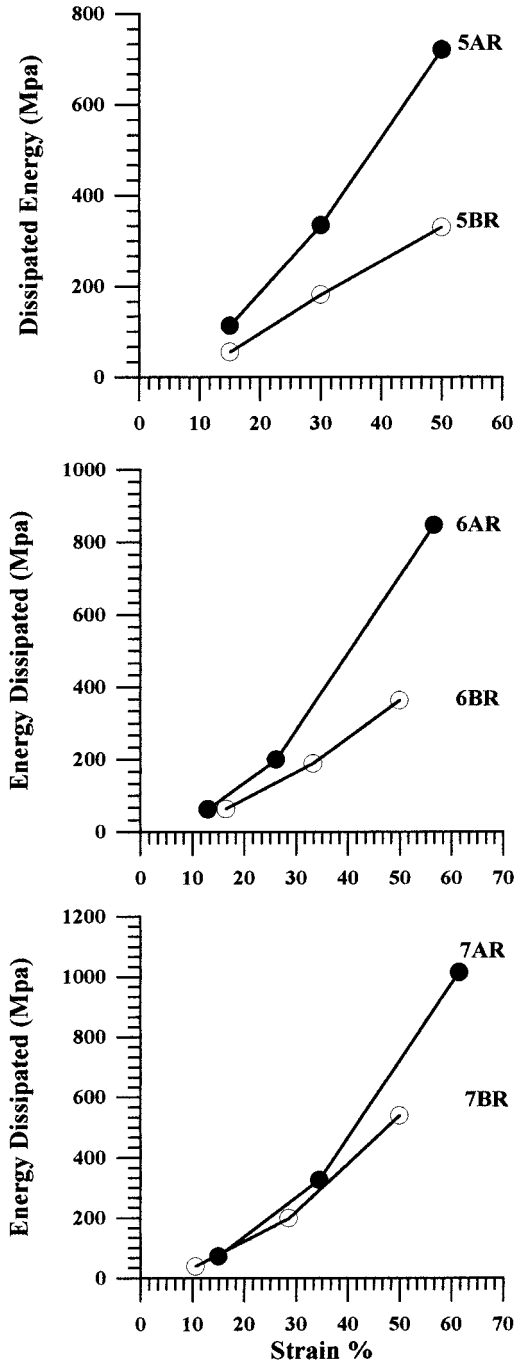

Figure 11. Dissipated energy (MPa) as a function of percent strain for fibers **A** (●) compared to fibers **B** (○).

Releasing the tension we observe the transition from the crystalline form III to either the helical form I or the oriented mesophase.

Elastic Behavior. We previously showed that the fibers, after releasing the tension, undergo a very large shrinkage defined as $(l_\lambda - l_1)/l_\lambda \times 100$, and in Table 1, we reported this value for all the fibers. In the interval between l_λ and l_1, we investigated the elastic behavior of the oriented samples, stretching the sample from the relaxed value of length l_1 up to the initial value of length l_λ. Figure 9 shows the hysteresis cycles for sample **7BR**, obtained by stretching the sample from l_λ to l_1 in three

steps and registering the stress during the increase and the decrease of the strain. The area of each hysteresis curve represents the energy dissipated during the cycle: it increases on increasing the strain, but the energy of dissipation, calculated from the area of each cycle (see Table 4) is quite low and the deformation is almost completely recoverable. In the table is also shown the permanent set, that is the residual deformation after each cycle: it is very low, reaching about 16% for the maximum strain. In any case, the initial length is completely recovered after 2 h of rest.

The hysteresis cycles are reported in Figure 10 for sample **7AR**. The elastic behavior is qualitatively very similar to the previous sample, but the energy dissipated and the permanent set are higher in this case. All the mechanical parameters are reported in Table 4.

In Figure 11, we report the dissipated energy as a function of the strain (%) for the fibers obtained from the two starting samples **A** and **B**. We can observe that the energy dissipated by the **BR** samples is always less than the **AR** samples; that is, the elastic behavior of the fibers drawn from the trans-planar mesophase is better than that of the fibers drawn from form I. Since the hysteresis is generally related to a crystallization phenomenon on drawing, it is reasonable that fibers of **A** type crystallize more easily, as X-rays also revealed.

In any case, the important point is that the two series of relaxed fibers, despite a different structural organization, show good elastic properties and the same qualitative behavior. Certainly the elasticity is driven by the large shrinkage of the fibers, which is a sign of the intrinsic instability of the drawn material. The appearance or the increase of the helical bands in the infrared spectra of the relaxed fibers could suggest that the contraction is due to a transition from the trans-planar to the helical conformation of molecules connecting different crystalline blocks along the fiber direction. The ratio of the *c* axis repeat distances of the two forms is 74%, making the observed contraction of 33−38% a little large and indicating that some additional mechanism is operative. Therefore, the explanation of the elasticity is very complex and cannot be simply related to the crystalline structure before and after releasing the tension.

Thermomechanical and morphological studies are in progress in our laboratory and we will show the results in a forthcoming paper.

Acknowledgment. This work was supported by Ministero dell'Università e della Ricerca Scientifica e Tecnologica (PRIN 1998 titled "Stereoselective Polymerization: New Catalyst and New Polymeric Materials")

References and Notes

(1) Ewen, J. A.; Jones, J. A.; Razavi, A.; Ferrara, J. D. *J. Am. Chem. Soc.* **1988**, *101*, 6255.
(2) Longo, P.; Proto, A.; Grassi, A.; Ammendola, P. *Macromolecules* **1992**, *24*, 462.
(3) Grisi, F.; Longo, P.; Zambelli, A.; Ewen, J. A. *J. Mol. Catal. A: Chem.* **1999**, *140*, 225.
(4) Lotz, B.; Lovinger, A. J.; Cais, R. E. *Macromolecules* **1988**, *21*, 2375.
(5) Lovinger A. J.; Lotz, B.; Cais, R. E. *Polymer* **1990**, *31*, 2253.
(6) Lovinger, A. J.; Davis, D. D.; Lotz, B. *Macromolecules* **1991**, *24*, 552.
(7) Lovinger, A. J.; Lotz, B.; Davis, D. D.; Padden, F. J. *Macromolecules* **1993**, *26*, 3494.
(8) Chatani, Y.; Maruyama, H.; Noguchi, K.; Asanuma, T.; Shiomura, T. *J Polym. Sci., Part C* **1990**, *28*, 393.
(9) Chatani, Y.; Maruyama, H.; Asanuma, T.; Shiomura, T. J. *J. Polym. Sci., Polym. Phys. Ed.* **1991,** *29*, 1649.
(10) De Rosa, C.; Corradini, P. *Macromolecules* **1993**, *26*, 5711.
(11) Auriemma, F.; Lewis, R. H.; Spiess, H. W.; De Rosa, C. *Macromol. Chem. Phys.* **1995**, *196*, 4011.
(12) De Rosa, C.; Auriemma, F.; Corradini, P. *Makromol. Chem.* **1996**, *29*, 7452.
(13) De Rosa, C.; Auriemma, F.; Vinti, V. *Macromolecules* **1997**, *30*, 4137.
(14) De Rosa, C.; Auriemma, F.; Vinti, V. *Macromolecules* **1998**, *31*, 7450.
(15) Lacks, D. J. *Macromolecules* **1996**, *29*, 1849.
(16) Palmo, K.; Krimm, S. *Macromolecules* **1996**, *29*, 8549.
(17) Uehara, H.; Yamazaki, Y.; Kanamoto, T. *Polymer* **1996**, *37*, 57.
(18) Loos, J.; Buhk, M.; Petermann, J.; Zoumis, K.; Kaminsky, W. *Polymer* **1996**, *37*, 387.
(19) Loos, J.; Petermann, J.; Waldofner, A. *Colloid Polym. Sci.* **1997**, *275*, 1088.
(20) Nakaoki, T.; Ohira, Y.; Hayashi, H. *Macromolecules* **1998**, *31*, 2705.
(21) Vittoria, V.; Guadagno, L.; Comotti, A.; Simonutti, R.; Auriemma, F.; De Rosa, C. *Macromolecules* **2000**, *33*, 6200.
(22) Loos, J.; Huckert, A.; Petermann, J. *Colloid Polym. Sci.* **1996**, *274*, 100.
(23) Guadagno, L.; D'Aniello, C.; Naddeo, C.; Vittoria, V. *Macromolecules* **2000**, *33*, 6023.
(24) D'Aniello, C.; Guadagno, L.; Naddeo, C.; Vittoria, V. *Macromol. Rapid Commun.* **2001**, *22*, 104.
(25) Loos, J.; Schimanski, T. *Polym Eng. Sci.* **2000**, *40*, 567.
(26) Noether, H. D.; Whitney, W. *Kolloid Z. Z. Polym.* **1973**, *251*, 991.
(27) Quynn, R. G.; Brody, H. *J. Macromol. Sci.—Phys.* **1971**, *B*, 721.
(28) Sprague, B. S. *J. Macromol. Sci.—Phys.* **1973**, *B*, 157.
(29) Cannon, S. L.; McKenna, G. B.; Statton, W. O. *J. Polym Sci., Macromol. Rev.* **1976**, *11*, 209.
(30) Guadagno, L.; Fontanella, C.; Vittoria, V.; Longo, P. *J. Polym. Sci., Part C* **1999**, *37*, 173.
(31) Treloar, L. R. G. *The Physics of Rubber Elasticity*; Clarendon Press: Oxford, England, 1973.
(32) Corradini, P.; Natta, G.; Ganis, P.; Temussi, P. *J. Polym. Sci. C* **1967**, *16*, 2477.
(33) Natta, G.; Corradini, P.; Ganis, P. *Makromol. Chem.* **1960**, *39*, 238.
(34) Hasegawa, R.; Takahashi, Y.; Chatani, Y.; Tadokoro, H. *Polym. J.* **1972**, *3*, 600.
(35) De Candia, F.; Russo, R.; Vittoria, V. *Polym. Commun.* **1991**, *32*, 306.

MA0019398